proceedings

ISEA 2018
Brisbane Queensland Australia
26-29 March 2018
'Engineering of Sport'

MDPI

Proceedings

Some Effects of Crosswind on the Lateral Dynamics of a Bicycle †

A. L. Schwab *, George Dialynas and Riender Happee

Biomechanical Engineering, Mechanical Engineering, Delft University of Technology, Mekelweg 2, 2628 CD Delft, The Netherlands; g.dialynas@tudelft.nl (G.D.); r.happee@tudelft.nl (R.H.)

* Correspondence: a.l.schwab@tudelft.nl; Tel.: +31-152-782-701

† Presented at the 12th Conference of the International Sports Engineering Association, Brisbane, Queensland, Australia, 26–29 March 2018.

Published: 24 February 2018

Abstract: The bicycle, being unstable at low speed and marginally stable at high speed, is sensitive to lateral perturbations. One of the major lateral perturbations is crosswind, which can lead to accidents and fatalities. Here we investigate the effect of crosswind on the lateral dynamics and control of the bicycle in a wide range of forward speeds and various crosswinds, by means of computer model analysis and simulation. A low dimensional bicycle model is used together with experimentally identified rider control parameters. The crosswind forces are obtained from a recent experimental study. Analysis and simulation show that crosswind decreases the stability of the bicycle and is clearly a safety issue.

Keywords: bicycle; crosswind; dynamics; control; stability; handling

1. Introduction

Aerodynamic drag in bicycling has been studied extensively, with the main goal to reduce drag and improve performance, see f.i. [1]. Only very few studies have been done on the effect of crosswind in bicycling, one the first being Godthelp et al. [2]. Nathan Barry et al. measured the effect of crosswinds and wheel selection on the aerodynamic behavior of a cyclist [3]. In competitive cycling the need for speed with less physical effort has lead researchers to study the aerodynamic drag interactions between cyclists in a team pursuit [4]. Belloli et al. investigated drafting effects between two cyclists by wind tunnel tests [5]. Blocken et al. investigated the upstream effect on the cyclist by a following car [6], and a motorcycle using computational fluid dynamics (CFD) simulations and wind tunnels tests [7]. Kyle et al. present a review on the history of aerodynamics in cycling and physical factors that influence performance [8].

Here we study the effect of crosswind on the lateral dynamics and control of the bicycle by means of analysis and simulation on a computational model. Crosswind is a lateral perturbation on bicycling. And the bicycle, being unstable at low speed and marginally stable at high speed, is very sensitive to such a lateral perturbation, so there is a clear safety issue here. Although the total number of accidents caused by crosswind is small (5%), the effect is large since the majority of these accidents lead to severe or fatal accidents [9].

This paper is organised as follows. After this introduction the methods for model analysis and simulation are described. Next some results of various cases are presented and discussed, and the paper ends with some conclusions.

2. Methods

To study the effect of crosswind on the dynamics and control of a bicycle three basic ingredients are needed: a bicycle model, crosswind data, and a bicycle rider controller. For the bicycle model the recently benchmarked, low dimensional, Whipple/Carvallo bicycle model [10] is used. This is a minimal, three-degree of freedom, model of a bicycle rider system that is still able to show realistic lateral dynamics. The lateral forces generated by the crosswind are obtained from a recent experimental study by Fintelman et al. [11]. They measured the aerodynamic forces on a full-scale bicycle with mannequin for a variety of crosswind angles ranging from 0 to 90 degrees in a wind tunnel. In order to study the effect of crosswind in the unstable forward speed range of the bicycle, a realistic rider control model is added to the bicycle model. The added controller is a linear steer torque controller with full state feedback, where the feedback gains were obtained experimentally from a system identification process on a real bicycle rider system, riding on a treadmill [12].

The effect of crosswind is studied by means of time series analysis on the models, which are obtained by numerical integration of the equations of motion. Although the lateral dynamics can be described by a set of linear differential equations [10], the large change in heading angle of the bicycle at a space-fixed wind speed angle, adds a nonlinear element to the analysis.

2.1. Bicycle Model

For the lateral bicycle dynamics, the low dimensional Whipple/Carvallo bicycle model is used. This model, as shown in Figure 1, is fully described and benchmarked by Meijaard et al. [10]. For small nominal motions of the upright position, the longitudinal and lateral motions are decoupled. The forward dynamics can be described by one degree of freedom, the forward speed v. Here we assume constant forward speed. The lateral dynamics can be described by two degrees of freedom: the roll angle of the rear frame, denoted by φ, and the steering angle between the rear frame and the front frame, denoted by δ. The linearized equations for the lateral motion, if the bicycle is moving at a constant forward velocity v, have the structure

$$\mathbf{M}\ddot{\mathbf{q}} + v\mathbf{C}_1\dot{\mathbf{q}} + (g\mathbf{K}_0 + v^2\mathbf{K}_2)\mathbf{q} = \mathbf{T}, \quad (1)$$

where $\mathbf{q} = [\varphi, \delta]^T$ is the vector of generalized coordinates, the degrees of freedom, $\mathbf{T} = [T_\varphi, T_\delta]^T$ is the vector of generalised forces, $\mathbf{M}$ is the mass matrix, $v\mathbf{C}_1$ is the non-symmetric velocity sensitivity matrix that is linear in the velocity, and $g\mathbf{K}_0 + v^2\mathbf{K}_2$ is the non-symmetric stiffness matrix that consists of a symmetric part that depends on gravity g and a second part that is quadratic in the forward velocity v. The generalised forces are T_φ, an externally applied roll moment to the rear frame and T_δ, an applied action-reaction steer torque between the front frame and the rear frame. Expressions for the entries of the matrices in terms of the 25 geometric and mass parameters of the bicycle can be found in [10]. Here we use the values as presented by Schwab [12], since for this specific bicycle and rider combination we are able to add, later on, experimentally determined rider control parameters.

Although the two degrees of freedom fully describe the dynamics of the bicycle, the kinematics of the bicycle, i.e., the position of the rear contact point P on the plane and the heading of the bicycle, described by the yaw angle of the rear frame ψ, are described by the following set of first order differential equations, $\dot{\psi} = \left(\frac{v^2\delta + c\dot{\delta}}{w}\right)\cos\varepsilon$, $\dot{x}_P = v\cos\psi$, and $\dot{y}_P = v\sin\psi$, with the wheelbase w, the front wheel trail c and the head angle ε, see Figure 1. Finally, the position of the front wheel contact point Q, which can be used for animation of the motion, can be calculated from the state variables and the kinematics as, $x_Q = x_P + w\cos\psi + c\delta\cos\varepsilon\sin\psi$, and $y_Q = y_P + w\sin\psi + c\delta\cos\varepsilon\cos\psi$.

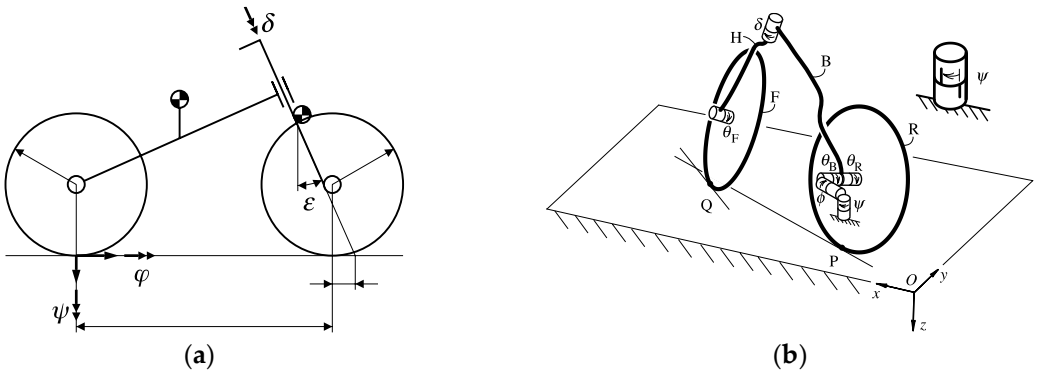

Figure 1. The low dimensional Whipple/Carvallo bicycle model with coordinates and main dimensions; (**a**) side view with rear frame roll angle φ, rear frame yaw angle ψ, front frame to rear frame steer angle δ, wheelbase w, front wheel trail c, and head angle ε, (**b**) 3D position and orientation of the bicycle model in the space fixed O-xyz coordinate system, with rear and front wheel contact points P and Q, figures from [13] and [10].

2.2. Cross Wind

For the aerodynamic forces the experimentally obtained data from Fintelman et al. [11] is used. They measured, in an open subsonic wind tunnel, the forces and moments exerted by the wind on a full-scale bicycle with mannequin. Measurements were done at a constant wind speed U_∞ of 9.91 m/s and for a variety of angles of attack β from 0 to 90 degrees. They present their results in the form of force and moment coefficients, CxA, such that the forces and moments can be calculated from $\frac{1}{2}\rho\, CxA\, v_a^2$, with the specific mass of the air ρ and the apparent total wind speed v_a. For a stationary bicycle $v_a = U_\infty$. For the lateral dynamics the side force and roll and yaw moment coefficients are important. These three coefficients determine the side force F_y and its point of application (x_s, z_s) in the bicycle plane (where the coordinate system of Figure 1 is used), as in

$$F_y = -\frac{1}{2}\rho\, CxA\, v_a^2, \qquad x_s = CyA/CsA + \frac{w}{2}, \qquad z_s = -CrA/CsA. \tag{2}$$

The side force F_y can be transformed to the applied generalised torques T_φ and T_δ, as used in the bicycle model, by means of the principle of virtual power. Or in other words, the virtual power of the side force is $F_y \delta\dot{y}_s$ should be equal to the virtual power of the applied generalised torques $T_\varphi \delta\dot{\varphi} + T_\delta \delta\dot{\delta}$ for arbitrary virtual generalised angular velocities $\delta\dot{\varphi}$ and $\delta\dot{\delta}$. The virtual velocity of the point of application of the side force in the y-direction is $\delta\dot{y}_s = -z_s\delta\dot{\varphi} + x_s\delta\dot{\psi}$, together with the kinematic equation for the yaw rate, $\dot{\psi}$, expressed in steer rate and steer angle, and keeping only virtual velocities, leads to $\delta\dot{y}_s = -z_s\delta\dot{\varphi} + x_s(c/w)\cos\varepsilon\,\delta\dot{\delta}$. Then the principle of virtual power results in the following expressions for the generalised torques due to crosswind,

$$T_\varphi = -CrA\,\frac{1}{2}\rho v_a^2, \qquad T_\delta = -(CyA + w/2\,CsA)(c/w)\cos\varepsilon\,\frac{1}{2}\rho v_a^2. \tag{3}$$

Unfortunately, Fintelman et al. [11] did not measure the reaction steer torque which kept the steering angle zero. For the crosswind it is assumed that absolute wind speed, with respect to the inertial coordinate system O-xyz, is constant in size, v_w and direction, α, see Figure 2c. The apparent wind speed with respect to the bicycle, v_a, is the vectorial sum of the absolute wind speed minus the forward speed of the bicycle. With the bicycle forward speed v, and bicycle heading ψ, the size and direction of the apparent wind speed with respect to the bicycle are,

$$v_a = \sqrt{v^2 + 2vv_w\cos(\alpha - \psi) + v_w^2}, \qquad \tan\beta = \frac{v_w\sin(\alpha - \psi)}{v + v_w\cos(\alpha - \psi)}. \tag{4}$$

Finally, with these values the aerodynamics coefficients, CxA, can be interpolated from Figures 3 and 6, as presented by Fintelman et al. [11], and the generalised applied torques (3) due to the crosswind can be calculated.

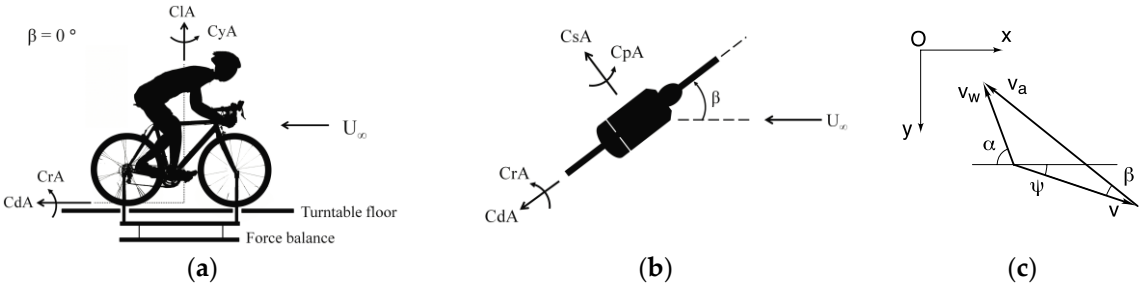

Figure 2. Bicycle and rider system subjected to cross wind together with the definition of the various aerodynamic force and moment coefficients and apparent wind speed, in (**a**) side view; and (**b**) top view, with drag force coefficient *CdA*, lift force coefficient *ClA*, side force coefficient *CsA*, roll moment coefficient *CrA*, pitch moment coefficient *CpA*, and yaw moment coefficient *CyA*; (**a**,**b**) from Fintelman et al. [11]; and (**c**) absolute wind speed v_w at an angle α, forward speed of the bicycle v at a heading ψ, and apparent wind speed v_a at an apparent angle β relative to the bicycle heading.

2.3. Time Series

For the time series analysis the set of second order differential equations describing the lateral dynamics (1) together with the differential equation for the heading are numerically integrated with a Runge-Kutta fourth order scheme with variable stepwise for local error control. For visualisation it can be useful to show the path of the contact points on the ground. Then the differential equations of the rear contact point can be added to system of differential equations. The path of the front contact point can finally be constructed from the state variables and kinematic equations, as presented in Section 2.1.

2.4. Rider Control

At low to moderate forward speed the bicycle is usually unstable and any lateral perturbation, like crosswind, will result in an unstable motion (fall to the ground). In order to investigate what the effect of crosswind is on the bicycle rider system, a rider controller is added to the system, stabilising the system at low forward speed. In previous work it has been shown that most of the rider control in bicycling is done by steering only [14]. Therefore, a steer torque controller with full state feedback is considered, where the feedback gains were obtained experimentally from a system identification process on a real bicycle rider system, riding on a treadmill [12]. This controller has the form, $T_\delta = \mathbf{K_c x}$, with the linear feedback gains $\mathbf{K_c}$, and the state vector $\mathbf{x} = (\dot{\varphi}, \dot{\delta}, \varphi, \delta, \psi)$. The feedback gains are scheduled for the specific forward speeds at hand. The values used in the simulation are represented in Appendix A, Table A1.

3. Results and Discussion

As a first example of the effect of crosswind on an uncontrolled bicycle two cases are considered. The first case is riding at a constant forward speed of v = 7.34 m/s (where the uncontrolled unperturbed bicycle is stable) in a crosswind with absolute wind speed v_w = 2.0 m/s at a wind speed angle of α = 30 degrees (Beaufort 2, light breeze). The analysis is done by means of a time series analysis, where the initial conditions on the bicycle are a zero roll and steer angle and zero roll and steer rate.

The path of the rear wheel contact point is shown in Figure 3a and shows that, after a short transient manoeuvre, the uncontrolled bicycle turns into the wind (the arrow indicates the wind direction). The transient behaviour of the roll and steer angle are shown in Figure 3b, where initially ($t < 1$ s) the crosswind force makes the bicycle steer to the left ($\delta < 0$) which makes the bicycle fall over to the right ($\varphi > 0$), this roll angle reverses the steering and makes the bicycle steer into the wind. The roll and steer angles settle to zero after about 25 s. This is in a light breeze and the maximum roll and steer angle are respectively 5.3 and 1.1 degree. In the second case all conditions remain the same, except for the wind speed, which is increased to v_w = 8.0 m/s. This corresponds to Beaufort 5, a fresh

breeze. Again, the uncontrolled bicycle turns into the wind but now the oscillatory behaviour persists for a much longer time, as shown in Figure 4. The maximum roll and steer angle are now much larger, respectively 30 and 7.5 degree. The mildly damped oscillation demonstrates the effect of the wind force on the lateral stability of the bicycle, and shows that an increasing wind speed reduces the stability of the system.

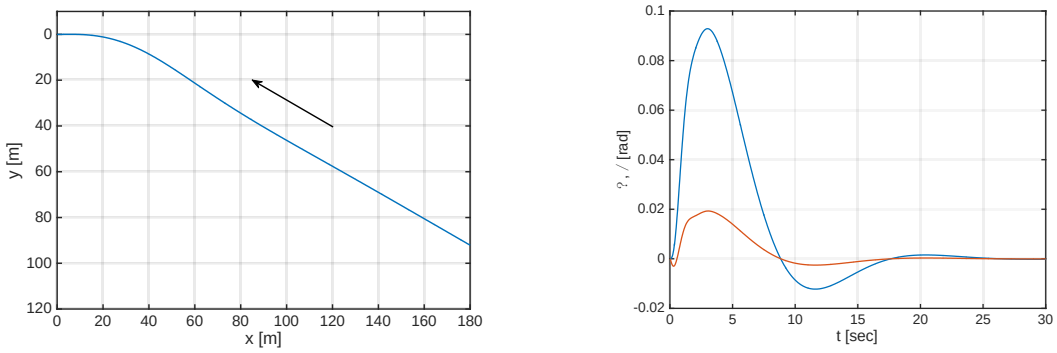

Figure 3. Time series of an uncontrolled bicycle running a constant forward speed of 7.34 m/s against a cross wind of 2.0 m/s at 30 degrees (Beaufort 2, light breeze); (**a**) path of the rear wheel contact point (arrow indicates the wind direction) (**b**) bicycle roll angle (blue) and steer angle (red) as a function of time.

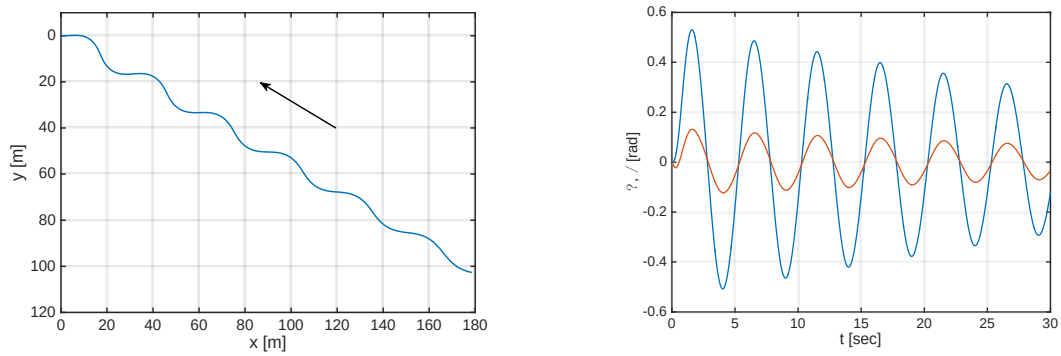

Figure 4. Time series of an uncontrolled bicycle running a constant forward speed of 7.34 m/s against a cross wind of 8.0 m/s at 30 degrees (Beaufort 5, fresh breeze); (**a**) path of the rear wheel contact point (arrow indicates the wind direction) (**b**) bicycle roll angle (blue) and steer angle (red) as a function of time.

As a last example, the effect of crosswind on a rider-controlled bicycle will be shown, by means of time series analysis. One case is considered, a low forward speed of v = 4.25 m/s, where the uncontrolled bicycle is unstable. A rider control model, as described in Section 2.4, is added to make the system stable. The control parameters are according to Table A1 from Appendix A. These rider control parameters where identified in an experiment where the rider was riding a bicycle on a treadmill [14]. Therefore, the controller not only tries to stabilise the bicycle, but also tries to keep the heading zero, otherwise one would run off the treadmill. The effect of crosswind with wind speed v_w = 10 m/s at a wind direction of α = 30 degrees; is considered, this is again Beaufort 5, a fresh breeze. After some initial transient response of about 10 s, the rider-controlled bicycle settles at a constant roll angle of 0.3 degrees at a zero steer angle, and a constant steer torque of 0.9 Nm, which is a considerable effort.

4. Conclusions

Crosswind in bicycling has a considerable effect on the stability and control of the bicycle. Our model simulations show that the tendency of an uncontrolled bicycle under the influence of

crosswind is to steer into the wind. In addition, crosswind can decrease the stable forward speed range of an uncontrolled bicycle, and with increasing wind speed can even make an initially stable uncontrolled bicycle, unstable for all forward speeds. Crosswind in a controlled bicycle increases the rider control effort considerably, due to a constant steer torque that has to be applied in order to keep the bicycle at a straight heading. These preliminary results clearly show that crosswind is a serious safety issue in bicycling.

Acknowledgments: We thank Danique Fintelman for her assistance in applying the aerodynamic forces to the model, and Nikhil Sharma for doing some initial calculations. This work has been funded by the FP7 Marie Curie programme (FP7-PEOPLE-2013-ITN) under grant agreement No. 608092.

Appendix A

Table A1. Mass, damping and stiffness matrices (1) for the bicycle model from Figure 1, together with some kinematic bicycle parameters; wheelbase w, front wheel trail c, head angle ε, and gravity acceleration g, and rider control feedback gains $\mathbf{K}_c$ for a forward speeds v; all in SI units, from [14].

$\mathbf{M}_0 = \begin{bmatrix} 133.31668525 & 2.43885691 \\ 2.43885691 & 0.22419262 \end{bmatrix}$, $\mathbf{C}_1 = \begin{bmatrix} 0 & 44.65783277 \\ -0.31500940 & 1.46189246 \end{bmatrix}$
$\mathbf{K}_0 = \begin{bmatrix} -116.73261635 & -2.48042260 \\ -2.48042260 & -0.77434358 \end{bmatrix}$, $\mathbf{K}_2 = \begin{bmatrix} 0 & 104.85805076 \\ 0 & 2.29688720 \end{bmatrix}$
$w = 1.0759$, $c = 0.0718$, $\varepsilon = 20.1$ degrees, $g = 9.81$ m/s^2
$\mathbf{K}c = [28.22, \quad -3.19, \quad 41.51, \quad -2.9979, \quad 47.8354]$, $v = 4.25$ m/s

References

1. Debraux, P.; Grappe, F.; Manolova, A.V.; Bertucci, W. Aerodynamic drag in cycling: Methods of assessment. *Sports Biomech.* **2011**, *10*, 197–218.
2. Godthelp, J.; Buist, M. *Stability and Manoeuvrability Characteristics of Single Track Vehicles*; Tech. Rep. IZF 1975 0-2; TNO Institute for Perception: Soesterberg, The Netherlands, 1975.
3. Barry, N.; Burton, D.; Crouch, T.; Sheridan, J.; Luescher, R. Effect of crosswinds and wheel selection on the aerodynamic behavior of a cyclist. *Procedia Eng*. **2012**, *34*, 20–25.
4. Barry, N.; Burton, D.; Sheridan, J.; Thompson, M.; Brown, N.A.T. Aerodynamic drag interactions between cyclists in a team pursuit. *Sports Eng.* **2015**, *18*, 93–103.
5. Belloli, M.; Giappino, S.; Robustelli, F.; Somaschini, C. Drafting Effect in Cycling: Investigation by Wind Tunnel Tests. *Procedia Eng.* **2016**, *147*, 38–43.
6. Blocken, B.; Toparlar, Y. A following car influences cyclist drag: CFD simulations and wind tunnel measurements. *J. Wind Eng. Ind. Aerodyn.* **2015**, *145*, 178–186.
7. Blocken, B.; Toparlar, Y.; Andrianne, T. Aerodynamic benefit for a cyclist by a following motorcycle. *J. Wind Eng. Ind. Aerodyn.* **2016**, *155*, 1–10.
8. Kyle, C.R.; Weaver, M.D. Aerodynamics of human-powered vehicles. *Proc. Inst. Mech. Eng. Part A J. Power Energy* **2004**, *218*, 141–154.
9. Schepers, P.; Wolt, K.K. Single-bicycle crash types and characteristics. *Cycl. Res. Int.* **2012**, *2*, 119–135.
10. Meijaard, J.P.; Papadopoulos, J.M.; Ruina, A.; Schwab, A.L. Linearized dynamics equations for the balance and steer of a bicycle: A benchmark and review. *Proc. R. Soc. A* **2007**, *463*, 1955–1982.
11. Fintelman, D.; Sterling, M.; Hemida, H.; Li, F.-X. The effect of crosswinds on cyclists: An experimental study. *Procedia Eng.* **2014**, *72*, 720–725.
12. Schwab, A.L.; de Lange, P.D.L.; Happee, R.; Moore, J.K. Rider control identification in bicycling using lateral force perturbation tests. *Proc. Inst. Mech. Eng. Part K J. Multi-Body Dyn.* **2013**, *227*, 390–406.
13. Meijaard, J.P. The loop closure equation for the pitch angle in bicycle kinematics. In Proceedings of the Bicycle and Motorcycle Dynamics 2013 Symposium on the Dynamics and Control of Single Track Vehicles, Narashino, Japan, 11–13 November 2013.
14. Moore, J.K.; Kooijman, J.D.G.; Schwab, A.L.; Hubbard, M. Rider motion identification during normal bicycling by means of principal component analysis. *Multibody Syst. Dyn.* **2011**, *25*, 225–244.